Leaky Rayleigh Wave Scattering From Elastic Media With Random Microstructures

By

Yuan Zhang and Richard L. Weaver

Department of Theoretical and Applied Mechanics

University of Illinois at Urbana-Champaign

Urbana, IL 61801

Abstract

We study the scattering of leaky Rayleigh wave from a flat fluid-solid interface. The fluid half-space is taken to be ideal and homogeneous while the solid half-space has randomly inhomogeneous anisotropic elastic constants due to the microstructure of the material. For plane waves incident from the fluid onto the interface at the critical Rayleigh angle the singly scattered incoherent field is obtained by utilizing a first Born approximation. When the solid is a crystal aggregate and when the correlation function is of exponential form, the mean square scattered signal level is found to be inversely proportional to the dimensionless frequency in the geometrical (high frequency) limit but proportional to the third power of frequency in the Rayleigh (low frequency) limit. Numerical results are given for water-aluminum (cubic polycrystals) interface scattering.

Introduction

Elastic surface waves have been studied for a long time after Lord Rayleigh and are well documented[1-8]. Early interest came mainly from seismologists because, by nature, surface waves propagate only in two-dimensions and their energy decays more slowly with increasing distance than that of bulk waves. Therefore, at large distance from the epicenter of an earthquake, damage at the surface of the earth is mainly caused by the surface waves[1]. Surface acoustic waves (SAW), defined by Oliner[9] as " ··· elastic waves of very high frequency that can be guided along the interface between two media, at least one of them being a solid," have also been used in signal processing. Possessing several advantages, surface wave delay lines and surface wave filters found many very important applications in radar, communications, and electronic warfare.

Surface wave techniques also play a very important role in nondestructive testing (NDT) and nondestructive evaluation (NDE)[9-19]. Owing to their propagation characteristics, surface acoustic waves, especially when acoustic energy is incident onto the interface at some critical angles[11], are very sensitive to discontinuities and changes of material properties at or near the surface and have been widely used for stress and texture measurement[11-15], surface flaw (microcracks or inclusions) detection[17-18], and interface characterization[19]. Surface wave techniques have many advantages compared to bulk wave measurements and can be used either to characterize structural materials directly or as an adjunct to bulk wave measurements. In addition to the case where only the surface features of the material are of interest, surface wave techniques can also be used for other cases such as: 1) if one can assume that the characteristics of the material near the surface adequately represent those of the bulk; 2) if the material geometry is too complex to use bulk wave measurements; 3) if material attenuation or thickness is too large; and 4) if one is interested in evaluating the differences between the bulk and surface layer properties.

Surface waves form an important part of the theory of wave propagation and scattering near medium interfaces. While the direct propagation study provides the foundation of surface wave devices, the inverse scattering investigation is the key to ultrasonic NDT / NDE. In the present paper, we study the problem of incoherent scattering of plane ultrasonic waves from a flat fluid-solid interface at the critical Rayleigh angle. The fluid is assumed to be homogeneous and ideal while the solid material is, due to its microstructure, inhomogeneous and anisotropic, though isotropic macroscopically. The ultrasonic field is expanded in powers of the material modulus heterogeneity and the relation between the mean square incoherently scattered signal level and the spectral density of the material inhomogeneities is established within the confines of the first Born (single scattering) approximation.

The single scattering approximation is expected to be accurate in the present case because of the features of the leaky surface wave. Since most of the energy carried by the surface wave in the solid will leak out into the fluid within a few wavelengths, it is reasonable to expect that most of the singly scattered energy will leak out before scattering again.

Sections I and II present the zeroth and first order solutions for the fields. The mean square incoherently scattered signal level as a function of the spectral density function of the medium moduli fluctuations is given in Section III. A special case of cubic crystal aggregates and exponential form of correlation function of the moduli fluctuations is discussed in Section IV and numerical results are presented in Section V.

I General Wave Equations and the Basic Zeroth Order Solution

Consider an inhomogeneous elastic half-space $z>0$, and a homogeneous ideal fluid half-space $z<0$, connected at $z = 0$. The elastic constants of the solid consist of two parts: a homogeneous, isotropic part plus a small randomly inhomogeneous, anisotropic variation part with zero mean. The density ρ_s of the solid is considered to be homogeneous. We consider only time harmonic waves, and write the reduced governing equations by omitting the harmonic time factor $e^{i\omega t}$. In the solid half-space they are

$$\begin{cases} \tau_{ij} = c_{ijkl} u_{k,l} \ , \\ \tau_{ij,j} + \rho_s \omega^2 u_i = 0 \ , \\ c_{ijkl} = \lambda_0 \delta_{ij}\delta_{kl} + \mu_0 (\delta_{ik}\delta_{jl} + \delta_{il}\delta_{jk}) + \varepsilon \Theta_{ijkl} \ , \end{cases} \tag{1}$$

where $0<\varepsilon<<1$, λ_0 and μ_0 are constants, ω is the angular frequency of the harmonic wave, and $\Theta_{ijkl} = \Theta_{ijkl}(x, y, z)$ are the components of a fourth order tensor which is a random function with zero mean.

Now define density ρ_f, and sound speed c_f for the fluid half-space in the region $z<0$, and expand the acoustic pressure in the fluid and the displacement in the solid in a Neumann series (also called the Born series)

$$P = P^0 + \varepsilon P^1 + \varepsilon^2 P^2 + \cdots, \qquad u_i = u_i^0 + \varepsilon u_i^1 + \varepsilon^2 u_i^2 + \cdots.$$

The zeroth order fields, which include the incident wave, satisfy the reduced wave equations

$$\begin{cases} \nabla^2 P^0 + k_f^2 P^0 = 0, & z<0, \\ (\lambda_0 + \mu_0)\, u^0_{k,ki} + \mu_0 u^0_{i,kk} + \rho_s \omega^2 u_i^0 = 0, & z>0, \end{cases} \tag{2}$$

where $k_f = \omega / c_f$. The interface continuity conditions for the zeroth order fields are

$$[u_z^0]\big|_{z=0} = 0, \qquad \tau_{zz}^0\big|_{z=0} = -P^0\big|_{z=0}, \qquad \tau_{xz}^0\big|_{z=0} = \tau_{yz}^0\big|_{z=0} = 0, \tag{2a}$$

The zeroth order stresses in the solid, as associated with the zeroth order displacements, are

$$\tau_{ij}^0 = \lambda_0 u_{k,k}^0 \delta_{ij} + \mu_0 (u_{i,j}^0 + u_{j,i}^0). \tag{2b}$$

The first order scattered wave fields satisfy

$$\begin{cases} \nabla^2 P^1 + k_f^2 P^1 = 0, & z<0, \\ (\lambda_0+\mu_0)\, u_{k,ki}^1 + \mu_0 u_{i,kk}^1 + \rho_s \omega^2 u_i^1 = -S_i, & z>0, \end{cases} \tag{3}$$

with a source term

$$S_i = (\Theta_{ijkl} u_{k,l}^0)_{,j}, \text{ or } \quad \underline{S} = \nabla \bullet [\Theta : (\nabla \underline{u}^0)], \tag{3a}$$

where Θ is for the fourth order tensor with components Θ_{ijkl}, and ":" represents a double dot product.

The continuity conditions at the interface $z = 0$ are still

$$[u_z^1]\big|_{z=0} = 0, \qquad \tau_{zz}^1\big|_{z=0} = -P^1\big|_{z=0}, \qquad \tau_{xz}^1\big|_{z=0} = \tau_{yz}^1\big|_{z=0} = 0, \tag{3b}$$

but since now

$$\tau_{ij}^1 = [\lambda_0 u_{k,k}^1 \delta_{ij} + \mu_0 (u_{i,j}^1 + u_{j,i}^1)] + [\Theta_{ijkl} u_{k,l}^0], \tag{3c}$$

there will be an extra source at the interface $z = 0$ for the first order fields.

We now consider a plane wave incident onto the solid at an angle θ_{in} from the z-axis, close to the Rayleigh angle $\theta_R = \arcsin(c_f/c_R)$, where c_R is the Rayleigh wave speed on a free surface. It may be noted that the complex speed c_{LR} of a leaky Rayleigh wave is determined by the appropriate complex root of the Leaky Rayleigh Function $F(k)$

$$F(k) = 4k^2 \eta_L \eta_T - (2k^2 - k_T^2)^2 + i(\rho_f/\rho_s) k_T^4 (\eta_L/\eta_f), \tag{4}$$

with $k = \omega/c$ and $\eta_{L,T} = \sqrt{k^2 - k_{L,T}^2}$, $\eta_f = \sqrt{k_f^2 - k^2}$. Usually $Re(c_{LR})$ is close to c_R and $Im(c_{LR})$ very small if the fluid density is small compared to that of the solid, i.e., $\rho_f \ll \rho_s$. It is well known that

$c_R < Re(c_{LR}) < c_T < c_L$.

Also in practice it is usually true that $c_f < c_R < Re(c_{LR})$.

The total zeroth order solution of (2), including the plane incident wave with a propagation vector $\vec{k}_0 = k_{0x}\hat{x} + k_{0y}\hat{y} + k_{0z}\hat{z} = k_f \sin\theta_{in}\cos\phi_{in}\hat{x} + k_f \sin\theta_{in}\sin\phi_{in}\hat{y} + k_f \cos\theta_{in}\hat{z}$ is, after using (2a),

$$\begin{cases} P^0 = e^{-i(k_{0x}x + k_{0y}y + k_{0z}z)} + [F^*(k_{0x}, k_{0y})/F(k_{0x}, k_{0y})]\, e^{-i(k_{0x}x + k_{0y}y - k_{0z}z)}, & z<0, \\ \underline{u}^0 = [\underline{U}(k_{0x}, k_{0y}; z)/\mu_0 F(k_{0x}, k_{0y})]\, e^{-i(k_{0x}x + k_{0y}y)}, & z>0, \end{cases} \tag{5}$$

where $F(k_x, k_y)$ is defined similar to Eq. (4) as

$$\begin{cases} F(k_x, k_y) = 4(k_x^2+k_y^2)\eta_L\eta_T - [2(k_x^2+k_y^2) - k_T^2]^2 + i(\rho_f/\rho_s)k_T^4(\eta_L/\eta_f) \ , \\ \eta_{L,T} = \sqrt{k_x^2+k_y^2-k_{L,T}^2} \ , \qquad \eta_f = \sqrt{k_f^2-(k_x^2+k_y^2)} = k_z \ . \end{cases} \tag{6}$$

and "*" denote the complex conjugate. $\underline{U}(k_x, k_y; z)$ is given by

$$\begin{cases} U_x(k_x, k_y; z) = -2ik_x[2(k_x^2+k_y^2) - k_T^2]e^{-\eta_L z} + i4k_x\eta_L\eta_T e^{-\eta_T z}, \\ U_y(k_x, k_y; z) = -2ik_y[2(k_x^2+k_y^2) - k_T^2]e^{-\eta_L z} + i4k_y\eta_L\eta_T e^{-\eta_T z}, \\ U_z(k_x, k_y; z) = -2\eta_L[2(k_x^2+k_y^2) - k_T^2]e^{-\eta_L z} + 4\eta_L(k_x^2+k_y^2)e^{-\eta_T z}, \end{cases} \tag{7}$$

The factors $\eta_{L,T}^0 = \sqrt{k_{0x}^2+k_{0y}^2-k_{L,T}^2} \approx \sqrt{[\omega/Re(c_{LR})]^2 - (\omega/c_{L,T})^2}$ are the z-decaying rates of the disturbance in the solid and are real and positive if the incident wave is, like the case here with $\theta_{in} \approx \theta_R$, outside the critical angles for transmission of L and T waves into the solid.

The disturbance described here is not, strictly speaking, a leaky Rayleigh wave. Such waves are usually defined as solutions to the case of no incident wave in the fluid and exponential decay in the x-y plane. In the limit that the fluid loading is modest and the incident angle is close to θ_R, the above solution is, however, closely related to the leaky Rayleigh wave.

This zeroth order solution represents the well understood case of a plane wave reflected from the interface between the fluid and the isotropic elastic half-space. We now study the first correction, which consists of waves which scatter only once from the microstructure of the solid.

II Dynamic Reciprocity Identity and the First Order Solution

Using Eq. (7), one can write the volume source term $\underline{S}$ in Eq. (2a) as

$$\underline{S}(\vec{r}; k_{0x}, k_{0y}) = [1/\mu_0 F(k_{0x}, k_{0y})] \nabla\bullet\{\Theta(\vec{r}) : [\nabla(\underline{U}(k_{0x}, k_{0y}; z)e^{-i(k_{0x}x + k_{0y}y)})]\} \tag{8}$$

The total first order solution of equations (3), (3a-c), and (8) can be obtained by inverting those equations directly. But it is more difficult to solve the equations with sources in the solid half-space than that with sources in the fluid half-space. In this section, we use the dynamic reciprocity identity to construct the first order solution from the above solution. We first derive the dynamic reciprocity identity suitable for our purpose here. Consider two cases:

Case A: Source in fluid

$$\begin{cases} \nabla^2 P^A + k_f^2 P^A = -F^A(\vec{r}, \vec{r}_A), & (z, z_A) < 0, \\ \tau_{ij,j}^A + \rho_s\omega^2 u_i^A = 0, & z > 0. \end{cases} \tag{9}$$

Case B: Source in Solid

$$\begin{cases} \nabla^2 P^B + k_f^2 P^B = 0, & z < 0, \\ \tau^B_{ij,j} + \rho_s \omega^2 u_i^B = -F_i{}^B(\vec{r}, \vec{r}_B), & (z, z_A) > 0. \end{cases} \tag{10}$$

For harmonic waves in an ideal fluid, we have

$u_i = (1/\rho_f \omega^2) P_{,i}$.

One can therefore write equations (9) and (10) as

$$\begin{cases} \rho_f c_f^2 \nabla (\nabla \bullet \underline{u}^A) + \rho_f \omega^2 \underline{u}^A = -k_f^{-2} \nabla F^A, & (z, z_A) < 0, \\ (\lambda_0 + 2\mu_0) \nabla (\nabla \bullet \underline{u}^A) - \mu_0 \nabla \times \nabla \times \underline{u}^A + \rho_s \omega^2 \underline{u}^A = 0, & z > 0, \end{cases} \tag{11}$$

and

$$\begin{cases} \rho_f c_f^2 \nabla (\nabla \bullet \underline{u}^B) + \rho_f \omega^2 \underline{u}^B = 0, & z < 0, \\ (\lambda_0 + 2\mu_0) \nabla (\nabla \bullet \underline{u}^B) - \mu_0 \nabla \times \nabla \times \underline{u}^B + \rho_s \omega^2 \underline{u}^B = -\underline{F}^B, & z, z_B > 0. \end{cases} \tag{12}$$

Thus the fluid can be considered here as a solid in the limit of vanishing shear modulus. We now use the dynamic reciprocity identity for linear elasticity[20, 21]

$$\int_0^t \iint_V \{ k_f^{-2} \nabla F^A(t-\tau) \bullet \underline{u}^B(\tau) - \underline{F}^B(t-\tau) \bullet \underline{u}^A(\tau) \} \, dV d\tau = \int_0^t \iint_{\partial V} \{ \underline{u}^A(t-\tau) \bullet \underline{T}^B(\tau) - \underline{u}^B(t-\tau) \bullet \underline{T}^A(\tau) \} \, dS d\tau , \tag{13}$$

where V is the volume of the medium (fluid and solid), ∂V is the surface of the volume, and $\underline{T}$ is the surface traction vector. Note that the interface ($z = 0$) is an inner surface of the system, the total virtual work done by the internal forces at this interface is zero, so ∂V of the surface integration on the RHS of (13) does not include this interface. We also use the relation

$$(\nabla F^A) \bullet \underline{u}^B = \nabla \bullet (F^A \underline{u}^B) - F^A (\nabla \bullet \underline{u}^B) ,$$

and the divergence theorem to write (13) as

$$\begin{aligned} &\int_0^t \iint_V \{ k_f^{-2} F^A(t-\tau) \nabla \bullet \underline{u}^B(\tau) + \underline{F}^B(t-\tau) \bullet \underline{u}^A(\tau) \} \, dV d\tau \\ &\qquad = -\int_0^t \iint_{\partial V} \{ \underline{u}^A(t-\tau) \bullet \underline{T}^B(\tau) - \underline{u}^B(t-\tau) \bullet \underline{T}^A - k_f^{-2} F^A(t-\tau) \underline{u}^B(\tau) \} \, dS d\tau . \end{aligned} \tag{14}$$

In the presence of infinitesimal damping one can always find a surface ∂V which is large enough that the disturbances from both sources A and B are negligible there. The RHS of (14) will be zero for this surface. Since the waves are harmonic, one can calculate the integration for τ and eliminate the common time factor, and then Eq. (14) becomes

$$\int_{-\infty}^{\infty} \{ k_f^{-2} F^A(\vec{r}) \nabla \bullet \underline{u}^B(\vec{r}) + \underline{F}^B(\vec{r}) \bullet \underline{u}^A(\vec{r}) \} \, d^3 r = 0. \tag{15}$$

We now let $F^A(\vec{r}) = \delta^3(\vec{r}-\vec{r}_A)$ and $\underline{F}^B(\vec{r}) = \underline{S}(\vec{r})$. Thus case B corresponds to equation (3) and case A is related to equation (2). We denote the corresponding displacement fields as $\underline{u}^A(\vec{r}, \vec{r}_A)$ and $\underline{u}^B(\vec{r}) = \underline{u}^1(\vec{r})$. Equation (15) becomes

$$u^1_{k,k}(\vec{r}_A) = -k_f^2 \int_{-\infty}^{\infty} \underline{S}(\vec{r}) \bullet \underline{u}^A(\vec{r}, \vec{r}_A)\, d^3r. \tag{16}$$

Using the relation

$$u^1_{k,k} = (1/\rho_f\omega^2) P^1_{,kk} = -(k_f^2/\rho_f\omega^2) P^1,$$

and changing $\vec{r}$ to $\vec{r}_s$, $\vec{r}_A$ to $\vec{r}$, we obtain

$$P^1(\vec{r}) = \rho_f\omega^2 \int_{-\infty}^{\infty} dx_s dy_s \int_0^{\infty} dz_s \underline{S}(\vec{r}_s) \bullet \underline{u}^A(\vec{r}_s, \vec{r}), \qquad z<0, \tag{17}$$

where $\underline{u}^A(\vec{r}, \vec{r}_A)$ is the displacement vector in the solid $(z>0)$ due to a point source in the fluid $(z_A<0)$, i.e., the solution of (9) when $F^A = \delta(x-x_A)\,\delta(y-y_A)\,\delta(z-z_A)$.

Case A of a point source in the fluid at a position $\vec{r}_A$ $(z_A<0)$ creates a field incident upon the solid representable as a superposition of plane waves

$$\left(\frac{1}{2\pi}\right)^2 \int dk_x dk_y \frac{1}{2ik_z} e^{-i(k_x x + k_y y + k_z z)}\, e^{i(k_x x_A + k_y y_A + k_z z_A)},$$

where $k_z = \sqrt{k_f^2 - k_x^2 - k_y^2} > 0$ and the integral is over only those (k_x, k_y) such that $k_x^2 + k_y^2 \le k_f^2$ because we have assumed that $k_f|z_A| \gg 1$ (far-field solution).

The response in the solid is therefore also representable as a similar superposition of plane wave responses (see Eq.(5))

$$\underline{u}^A(\vec{r}, \vec{r}_A) = \left(\frac{1}{2\pi}\right)^2 \int_{-\infty}^{\infty} dk_x dk_y \frac{e^{-i(k_x x + k_y y)}}{2i\mu_0 k_z F(k_x, k_y)} \underline{U}(k_x, k_y; z)\, e^{i(k_x x_A + k_y y_A + k_z z_A)}, \qquad z>0,\ z_A<0. \tag{18}$$

Note that the solution of case A, i.e. Eq. (18) does not apply when the source is at the interface. This is because we have used the stress continuity conditions at the interface in obtaining the solution. In fact, stresses are continuous at the interface only when the source is not at the interface. One has to make careful analysis to obtain an uniformly valid solution to include the interface source case and this is not a simple task (see, for example, Maradudin and Mills[22], and Kaganova and Maradudin[23]). So instead of trying to find such an uniformly valid solution, we reconsider the problem from physical point of view.

Suppose we carefully coat a very thin homogeneous layer on the surface of the solid. Because the layer is homogeneous, $\Theta \equiv 0$ inside this thin layer and is unaltered on the interior of the solid half-space. If the layer is very thin, with thickness much smaller than either the average grain size or the shortest wavelength, then the physics of the problem will not be changed but the mathematics will be greatly simplified.

Now we can use Eq. (18) to formulate our solution because, by our assumption made above, $\Theta \equiv 0$ at the interface anyway. Also because of this same assumption, the extra interface source term mentioned before in Eq. (3c) will vanish.

Therefore, using Eqs. (17) and (18), one may write

$$P^1(\vec{r}) = \frac{\rho_f \omega^2}{(2\pi)^2} \int_{-\infty}^{\infty} dx_s dy_s \int_0^{\infty} dz_s \left[\int_{-\infty}^{\infty} dk_x dk_y \frac{e^{-i(k_x x_s + k_y y_s)}}{2i\mu_0 k_z F(k_x, k_y)} \underline{U}(k_x, k_y; z_s)\, e^{i(k_x x + k_y y + k_z z)} \right] \bullet \underline{S}(\vec{r}_s). \tag{19}$$

Using expression (8) for the volume source term, one has

$$\begin{aligned} P^1(\vec{r}) &= \frac{\rho_f \omega^2}{(2\pi)^2} \int_{-\infty}^{\infty} dx_s dy_s \int_0^{\infty} dz_s \left[\int_{-\infty}^{\infty} dk_x dk_y \frac{e^{i(k_x x + k_y y + k_z z)}}{2ik_z} \frac{\underline{U}(k_x, k_y; z_s)\, e^{-i(k_x x_s + k_y y_s)}}{\mu_0 F(k_x, k_y)} \right] \\ &\quad \bullet \left[\frac{\nabla_s \bullet \{ \Theta(\vec{r}_s) : [\, \nabla_s (\underline{U}(k_{0x}, k_{0y}; z_s)\, e^{-i(k_{0x} x_s + k_{0y} y_s)})] \}}{\mu_0 F(k_{0x}, k_{0y})} \right] \\ &= \frac{\rho_f \omega^2}{(2\pi)^2} \int_{-\infty}^{\infty} dk_x dk_y \frac{e^{i(k_x x + k_y y + k_z z)}}{2ik_z} \int_{-\infty}^{\infty} dx_s dy_s \int_0^{\infty} dz_s \left[\frac{\underline{U}(k_x, k_y; z_s)\, e^{-i(k_x x_s + k_y y_s)}}{\mu_0 F(k_x, k_y)} \right] \\ &\quad \bullet \left[\frac{\nabla_s \bullet \{ \Theta(\vec{r}_s) : [\, \nabla_s (\underline{U}(k_{0x}, k_{0y}; z_s)\, e^{-i(k_{0x} x_s + k_{0y} y_s)})] \}}{\mu_0 F(k_{0x}, k_{0y})} \right] \end{aligned} \tag{20}$$

where "∇_s" indicates that the differentiation is on (x_s, y_s, z_s).

Eq. (20) constitutes an expression for the first order, singly scattered field in the fluid in terms of the modulus fluctuations Θ_{ijkl} of the solid. The expression may be simplified by using Green's integral theorem to write the integral as

$$\begin{aligned} &\int dV_s \, [\underline{U}(k_x, k_y; z_s)\, e^{-i(k_x x_s + k_y y_s)}] \bullet [\, \nabla_s \bullet \{ \Theta(\vec{r}_s) : [\, \nabla_s (\underline{U}(k_{0x}, k_{0y}; z_s)\, e^{-i(k_{0x} x_s + k_{0y} y_s)})] \} \,] \\ &\quad = \oint [\underline{U}(k_x, k_y; z_s)\, e^{-i(k_x x_s + k_y y_s)}] \bullet [\, \Theta(\vec{r}_s) : \{ \nabla_s (\underline{U}(k_{0x}, k_{0y}; z_s)\, e^{-i(k_{0x} x_s + k_{0y} y_s)}) \}] \bullet d\vec{A} \\ &\quad - \int dV_s \, [\, \nabla_s \{ \underline{U}(k_x, k_y; z_s)\, e^{-i(k_x x_s + k_y y_s)} \} \,] : \Theta(\vec{r}_s) : [\, \nabla_s \{ \underline{U}(k_{0x}, k_{0y}; z_s)\, e^{-i(k_{0x} x_s + k_{0y} y_s)} \}], \end{aligned} \tag{21}$$

The integral over V_s is confined to the solid half-space, $z \geq 0$. The surface integral is over the interface, $d\vec{A} = -\hat{z} dx dy$, and is zero from the assumption $\Theta_{ijkl}(x, y, z = 0) = 0$ made above.

The volume integral in Eq. (21) is symmetric with respect to the incoming $\vec{k}_{in} = \vec{k}_0$ and the

outgoing $\hat{k}$ directions. This symmetry reflects acoustic reciprocity.

Now one can write (20) as

$$P^1(\hat{r}) = -\frac{\rho_f \omega^2}{(2\pi)^2 2i\mu_0^2} \int_{-\infty}^{\infty} dk_x dk_y \frac{e^{i(k_x x + k_y y + k_z z)}}{F(k_x, k_y) F(k_{0x}, k_{0y}) k_z} \times \int_{-\infty}^{\infty} dx_s dy_s \int_0^{\infty} dz_s \left[U_i(k_x, k_y; z_s) e^{-i(k_x x_s + k_y y_s)}\right]_{,j} \Theta_{ijkl}(x_s, y_s, z_s) \left[U_k(k_{0x}, k_{0y}; z_s) e^{-i(k_{0x} x_s + k_{0y} y_s)}\right]_{,l}. \quad (22)$$

By changing (k_x, k_y) to $(-k_x, -k_y)$ (notice that the sign of k_z is unchanged and that $F(-k_x, -k_y) = F(k_x, k_y)$), Eq. (22) reads

$$P^1(\hat{r}) = -\frac{\rho_f \omega^2}{(2\pi)^2 2i\mu_0^2} \int_{-\infty}^{\infty} dk_x dk_y \frac{e^{ik_z z} e^{-i(k_x x + k_y y)}}{F(k_x, k_y) F(k_{0x}, k_{0y}) k_z} \times \int_{-\infty}^{\infty} dx_s dy_s \int_0^{\infty} dz_s \left[U_i(-k_x, -k_y; z_s) e^{i(k_x x_s + k_y y_s)}\right]_{,j} \Theta_{ijkl}(x_s, y_s, z_s) \left[U_k(k_{0x}, k_{0y}; z_s) e^{-i(k_{0x} x_s + k_{0y} y_s)}\right]_{,l}. \quad (23)$$

We now define the Fourier transform pairs as

$$\mathcal{FT}_2(f) = \tilde{f}(k_x, k_y; z) = \int_{-\infty}^{\infty} dx dy e^{i(k_x x + k_y y)} f(x, y, z), \qquad f(x, y, z) = \left(\frac{1}{2\pi}\right)^2 \int_{-\infty}^{\infty} dk_x dk_y e^{-i(k_x x + k_y y)} \tilde{f}(k_x, k_y; z),$$

in two-dimensions, and

$$\begin{cases} \mathcal{FT}_3(f) = \tilde{f}(k_x, k_y, k_z) = \int_{-\infty}^{\infty} dx dy dz e^{i(k_x x + k_y y + k_z z)} f(x, y, z), \\ f(x, y, z) = \left(\frac{1}{2\pi}\right)^3 \int_{-\infty}^{\infty} dk_x dk_y dk_z e^{-i(k_x x + k_y y + k_z z)} \tilde{f}(k_x, k_y, k_z), \end{cases}$$

in three-dimensions.

Through the above definition of inverse Fourier transform, one may recognize that

$$\tilde{P}^1(k_x, k_y; z) = -\frac{\rho_f \omega^2}{2i\mu_0^2} \frac{e^{ik_z z}}{F(k_x, k_y) F(k_{0x}, k_{0y}) k_z} \times \int_{-\infty}^{\infty} dx_s dy_s \int_0^{\infty} dz_s \left[U_i(-k_x, -k_y; z_s) e^{i(k_x x_s + k_y y_s)}\right]_{,j} \Theta_{ijkl}(x_s, y_s, z_s) \left[U_k(k_{0x}, k_{0y}; z_s) e^{-i(k_{0x} x_s + k_{0y} y_s)}\right]_{,l}. \quad (24)$$

One also notices that the integrals in (24) are of Fourier transform form. For example,

$$\int_{-\infty}^{\infty} dx_s dy_s U_i(-k_x, -k_y; z_s) e^{i(k_x x_s + k_y y_s)} \Theta_{i3k1}(x_s, y_s, z_s) \left[U_k(k_{0x}, k_{0y}; z_s) e^{-i(k_{0x} x_s + k_{0y} y_s)}\right]_{,x_s}$$

$$= -ik_{0x} U_i(-k_x, -k_y; z_s) U_k(k_{0x}, k_{0y}; z_s) \tilde{\Theta}_{i3k1}(k_x - k_{0x}, k_y - k_{0y}; z_s),$$

where $\tilde{\Theta}_{ijkl}(k_x, k_y; z)$ is the two-dimensional Fourier transform of $\Theta_{ijkl}(x, y, z)$.

After some manipulation, one can rewrite Eq. (24) as

$$\tilde{P}^1(k_x, k_y; z) = \frac{\rho_f \omega^2}{2i\mu_0^2} \frac{e^{ik_z z}}{F(k_x, k_y) F(k_{0x}, k_{0y}) k_z}$$

$$\times \{ -k_{0\alpha} k_\beta \int_0^\infty dz_s J_{ij}^{00}(k_{0x}, k_{0y}; k_x, k_y; z_s) \tilde{\Theta}_{ij\alpha\beta}(k_x - k_{0x}, k_y - k_{0y}; z_s)$$

$$-ik_\alpha \int_0^\infty dz_s J_{ij}^{01}(k_{0x}, k_{0y}; k_x, k_y; z_s) \tilde{\Theta}_{ij\alpha 3}(k_x - k_{0x}, k_y - k_{0y}; z_s) \qquad (25)$$

$$+ik_{0\alpha} \int_0^\infty dz_s J_{ij}^{10}(k_{0x}, k_{0y}; k_x, k_y; z_s) \tilde{\Theta}_{ij\alpha 3}(k_x - k_{0x}, k_y - k_{0y}; z_s)$$

$$-\int_0^\infty dz_s J_{ij}^{11}(k_{0x}, k_{0y}; k_x, k_y; z_s) \tilde{\Theta}_{ij33}(k_x - k_{0x}, k_y - k_{0y}; z_s) \quad \}.$$

with summation of (α, β) over 1 and 2 (or x and y), summation of (i, j) 1 through 3, and with

$$J_{ij}^{MN}(k_{0x}, k_{0y}; k_x, k_y; z_s) = U_i^{(M)}(-k_x, -k_y; z_s) U_j^{(N)}(k_{0x}, k_{0y}; z_s) \qquad (M, N) = 0, 1 \qquad (25a)$$

where $U^{(M)} = \partial^M U / \partial z^M$. In writing Eq. (25), we have also utilized the fact that Θ_{ijkl} is symmetric between i and j, or k and l.

III Mean Square Incoherently Singly Scattered Signal Level

Now consider the averaged signal intensity of the singly scattered waves in any direction $\hat{n} = n_x\hat{x} + n_y\hat{y} + n_z\hat{z}$ other than the specular direction at which the signal is contaminated by the less interesting coherent reflections. We assume that a receiver with a narrow beam pattern is placed in the far field at $z < 0$, with its beam oriented towards the scatterer in the "listening direction" $\hat{n}$. We denote by T the receiver's sensitivity which is a function of the angle between the direction $\hat{k} = \vec{k}/k_0$ of the plane wave component $\tilde{P}(\vec{k})$ and the receiver beam axis $\hat{n}$, i.e., a function of $\hat{n} \bullet \hat{k}$. The received signal is then

$$V(\hat{n}) = \int_{-\infty}^{\infty} dk_x dk_y \tilde{P}(k_x, k_y) T(\hat{n} \bullet \hat{k}). \qquad (26)$$

The ensemble averaged "intensity" of the signal, the so called "mean square signal level", is then given by

$$<|V(\hat{n})|^2> = \int_{-\infty}^{\infty} dk_{1x}dk_{1y} \int_{-\infty}^{\infty} dk_{2x}dk_{2y} <\tilde{P}(k_{1x}, k_{1y}) \tilde{P}^*(k_{2x}, k_{2y})> T(\hat{n} \bullet \hat{k}_1)\, T^*(\hat{n} \bullet \hat{k}_2) \quad . \tag{27}$$

From (25), one has

$$<\tilde{P}^1(k_{1x}, k_{1y}; z)\ \tilde{P}^{1*}(k_{2x}, k_{2y}; z)> = \left(\frac{\rho_f \omega^2}{2\mu_0^2}\right)^2 \frac{e^{i(k_{1z}-k_{2z})z} I(k_{0x}, k_{0y}; k_{1x}, k_{1y}; k_{2x}, k_{2y})}{F(k_{1x}, k_{1y})\ F^*(k_{2x}, k_{2y})\,|\,F(k_{0x}, k_{0y})|^2 k_{1z}k_{2z}} \quad , \tag{28}$$

where " * " denotes the complex conjugate and

$I(k_{0x}, k_{0y}; k_{1x}, k_{1y}; k_{2x}, k_{2y})$

$$\begin{aligned}
&= k_{0\alpha}k_{0\gamma}k_{1\beta}k_{2\delta} \int_0^{\infty} dz_1 \int_0^{\infty} dz_2 J_{ij}^{00}(k_{0x}, k_{0y}; k_{1x}, k_{1y}; z_1)\, J_{kl}^{00*}(k_{0x}, k_{0y}; k_{2x}, k_{2y}; z_2) <\tilde{\Theta}_{ij\alpha\beta}(z_1)\, \tilde{\Theta}^*_{kl\gamma\delta}(z_2)> \\
&\quad + k_{2\alpha}k_{2\beta} \int_0^{\infty} dz_1 \int_0^{\infty} dz_2 J_{ij}^{01}(k_{0x}, k_{0y}; k_{1x}, k_{1y}; z_1)\, J_{kl}^{01*}(k_{0x}, k_{0y}; k_{2x}, k_{2y}; z_2) <\tilde{\Theta}_{ij\alpha 3}(z_1)\, \tilde{\Theta}^*_{kl\beta 3}(z_2)> \\
&\quad + k_{0\alpha}k_{0\beta} \int_0^{\infty} dz_1 \int_0^{\infty} dz_2 J_{ij}^{10}(k_{0x}, k_{0y}; k_{1x}, k_{1y}; z_1)\, J_{kl}^{10*}(k_{0x}, k_{0y}; k_{2x}, k_{2y}; z_2) <\tilde{\Theta}_{ij\alpha 3}(z_1)\, \tilde{\Theta}^*_{kl\beta 3}(z_2)> \\
&\quad + \int_0^{\infty} dz_1 \int_0^{\infty} dz_2 J_{ij}^{11}(k_{0x}, k_{0y}; k_{1x}, k_{1y}; z_1)\, J_{kl}^{11*}(k_{0x}, k_{0y}; k_{2x}, k_{2y}; z_2) <\tilde{\Theta}_{ij33}(z_1)\, \tilde{\Theta}^*_{kl33}(z_2)> \qquad (28a) \\
&\quad + 2Re\left[-ik_{0\alpha}k_{2\beta}k_{2\gamma} \int_0^{\infty} dz_1 \int_0^{\infty} dz_2 J_{ij}^{00}(k_{0x}, k_{0y}; k_{1x}, k_{1y}; z_1)\, J_{kl}^{01*}(k_{0x}, k_{0y}; k_{2x}, k_{2y}; z_2) <\tilde{\Theta}_{ij\alpha\beta}(z_1)\, \tilde{\Theta}^*_{kl\gamma 3}(z_2)>\right] \\
&\quad + 2Re\left[ik_{0\alpha}k_{0\gamma}k_{1\beta} \int_0^{\infty} dz_1 \int_0^{\infty} dz_2 J_{ij}^{00}(k_{0x}, k_{0y}; k_{1x}, k_{1y}; z_1)\, J_{kl}^{10*}(k_{0x}, k_{0y}; k_{2x}, k_{2y}; z_2) <\tilde{\Theta}_{ij\alpha\beta}(z_1)\, \tilde{\Theta}^*_{kl\gamma 3}(z_2)>\right] \\
&\quad + 2Re\left[k_{0\alpha}k_{1\beta} \int_0^{\infty} dz_1 \int_0^{\infty} dz_2 J_{ij}^{00}(k_{0x}, k_{0y}; k_{1x}, k_{1y}; z_1)\, J_{kl}^{11*}(k_{0x}, k_{0y}; k_{2x}, k_{2y}; z_2) <\tilde{\Theta}_{ij\alpha\beta}(z_1)\, \tilde{\Theta}^*_{kl33}(z_2)>\right] \\
&\quad + 2Re\left[-k_{0\beta}k_{1\alpha} \int_0^{\infty} dz_1 \int_0^{\infty} dz_2 J_{ij}^{01}(k_{0x}, k_{0y}; k_{1x}, k_{1y}; z_1)\, J_{kl}^{10*}(k_{0x}, k_{0y}; k_{2x}, k_{2y}; z_2) <\tilde{\Theta}_{ij\alpha 3}(z_1)\, \tilde{\Theta}^*_{kl\beta 3}(z_2)>\right] \\
&\quad + 2Re\left[ik_{1\alpha} \int_0^{\infty} dz_1 \int_0^{\infty} dz_2 J_{ij}^{01}(k_{0x}, k_{0y}; k_{1x}, k_{1y}; z_1)\, J_{kl}^{11*}(k_{0x}, k_{0y}; k_{2x}, k_{2y}; z_2) <\tilde{\Theta}_{ij\alpha 3}(z_1)\, \tilde{\Theta}^*_{kl33}(z_2)>\right] \\
&\quad + 2Re\left[ik_{0\alpha} \int_0^{\infty} dz_1 \int_0^{\infty} dz_2 J_{ij}^{10}(k_{0x}, k_{0y}; k_{1x}, k_{1y}; z_1)\, J_{kl}^{11*}(k_{0x}, k_{0y}; k_{2x}, k_{2y}; z_2) <\tilde{\Theta}_{ij\alpha 3}(z_1)\, \tilde{\Theta}^*_{kl33}(z_2)>\right],
\end{aligned}$$

where

$$<\tilde{\Theta}_{ij\alpha\beta}(z_1)\, \tilde{\Theta}^*_{kl\gamma\delta}(z_2)> \equiv <\tilde{\Theta}_{ij\alpha\beta}(k_{1x}, k_{1y}; z_1)\, \tilde{\Theta}^*_{kl\gamma\delta}(k_{2x}, k_{2y}; z_2)>. \tag{28b}$$

Summation of $(\alpha, \beta, \gamma, \delta)$ in the above equations is over 1 and 2 (or x and y) and summation of (i, j, k, l) is over 1 through 3 (or x,y and z).

Consider the case where the solid is a crystal aggregate. We make use of two common assumptions[24]: 1) there is no orientation correlation between different crystallites, and 2) the polycrystal's second order statistics are homogeneous and isotropic. The first one is equivalent to the assumption that the tensorial character of the covariance functions decouples from the spatial dependence. The second assumption states that the covariance functions are functions of $|\hat{r}-\hat{r}'|$ rather than $\hat{r}$ and $\hat{r}'$ separately. Under these two standard assumptions, one has

$$<\Theta_{mnpq}(x_1, y_1, z_1)\,\Theta^*_{ijkl}(x_2, y_2, z_2)> \;=\; \Xi^{mnpq}_{ijkl}\; R_\Theta(|\hat{r}_1-\hat{r}_2|) \tag{29}$$

where Ξ^{mnpq}_{ijkl} is an eighth rank constant tensor depending on the microstructure of the crystal. The statistical homogeneity implies

$$\begin{aligned}&<\tilde{\Theta}_{mnpq}(k_{1x}, k_{1y}, k_{1z})\,\tilde{\Theta}^*_{ijkl}(k_{2x}, k_{2y}, k_{2z})>\\ &\qquad = (2\pi)^3\delta(k_{1x}-k_{2x})\,\delta(k_{1y}-k_{2y})\,\delta(k_{1z}-k_{2z})\,\Xi^{mnpq}_{ijkl}\;\tilde{R}_\Theta(k_{1x}, k_{1y}, k_{1z}),\end{aligned} \tag{29a}$$

for the three-dimension Fourier transforms, and

$$\begin{aligned}&<\tilde{\Theta}_{mnpq}(k_{1x}, k_{1y}; z_1)\,\tilde{\Theta}^*_{ijkl}(k_{2x}, k_{2y}; z_2)>\\ &\qquad = (2\pi)^2\delta(k_{1x}-k_{2x})\,\delta(k_{1y}-k_{2y})\;\;\Xi^{mnpq}_{ijkl}\;\tilde{R}_\Theta(k_{1x}, k_{1y}; z_1-z_2)\\ &\qquad = (2\pi)\,\delta(k_{1x}-k_{2x})\,\delta(k_{1y}-k_{2y})\;\;\Xi^{mnpq}_{ijkl}\int_{-\infty}^{\infty} d\xi\, e^{-i\xi(z_1-z_2)}\tilde{R}_\Theta(k_{1x}, k_{1y}, \xi),\end{aligned} \tag{29b}$$

for the two-dimension transforms. We substitute (29b) into Eqs. (28) and (28a) to obtain

$$\begin{cases}<\tilde{P}^1(k_{1x}, k_{1y}; z)\;\tilde{P}^{1*}(k_{2x}, k_{2y}; z)> = \mathcal{PP}\;\delta(k_{1x}-k_{2x})\,\delta(k_{1y}-k_{2y}) \;\;,\\ \mathcal{PP} = \left(\dfrac{\pi\rho_f^2\omega^4}{2\mu_0^4}\right)\dfrac{\displaystyle\int_{-\infty}^{\infty} d\xi\;\tilde{R}_\Theta(k_{1x}-k_{0x}, k_{1y}-k_{0y}, \xi)\,I^\Theta(\hat{k}_0, \hat{k}_1, \xi)}{k_{1z}k_{2z}\;F(k_{1x}, k_{1y})\;F^*(k_{2x}, k_{2y})\,|F(k_{0x}, k_{0y})|^2}\;\;,\end{cases} \tag{30}$$

with

$$\begin{aligned}I^\Theta(\hat{k}_0, \hat{k}, \xi) \;=\; & k_{0\alpha}k_{0\gamma}k_\beta k_\delta\;\Xi^{ij\alpha\beta}_{kl\gamma\delta}\;\mathcal{J}^{ijkl}_{0000} + k_\alpha k_\beta\;\Xi^{ij\alpha 3}_{kl\beta 3}\;\mathcal{J}^{ijkl}_{0101} + k_{0\alpha}k_{0\beta}\;\Xi^{ij\alpha 3}_{kl\beta 3}\;\mathcal{J}^{ijkl}_{1010} + \Xi^{ij33}_{kl33}\;\mathcal{J}^{ijkl}_{1111}\\ & + 2Re\,[-ik_{0\alpha}k_\beta k_\gamma\;\Xi^{ij\alpha\beta}_{kl\gamma 3}\;\mathcal{J}^{ijkl}_{0001} + ik_{0\alpha}k_{0\gamma}k_\beta\;\Xi^{ij\alpha\beta}_{kl\gamma 3}\;\mathcal{J}^{ijkl}_{0010} + k_{0\alpha}k_\beta\;\Xi^{ij\alpha\beta}_{kl33}\;\mathcal{J}^{ijkl}_{0011}]\\ & + 2Re\,[-k_\alpha k_{0\beta}\;\Xi^{ij\alpha 3}_{kl\beta 3}\;\mathcal{J}^{ijkl}_{0110} + ik_\alpha\;\Xi^{ij\alpha 3}_{kl33}\;\mathcal{J}^{ijkl}_{0111} + ik_{0\alpha}\;\Xi^{ij\alpha 3}_{kl33}\;\mathcal{J}^{ijkl}_{1011}],\end{aligned} \tag{30a}$$

where $\alpha, \beta = 1, 2$ or x, y, $i, j, k, l = 1, 2, 3$ or x, y, z, and $\mathcal{J}^{ijkl}_{MNPQ}$ is defined as

$$\mathcal{J}^{ijkl}_{MNPQ} = \int_0^\infty dz_1 J^{MN}_{ij}(k_x, k_y; z_1)\,e^{-i\xi z_1}\int_0^\infty dz_2 J^{PQ*}_{kl}(k_x, k_y; z_2)\,e^{i\xi z_2}\;\;, \tag{30b}$$

with $M, N, P, Q = 0, 1$.

If one considers only the singly scattered waves and substitutes (30) into (27), one has

$$<|V(\hat{n})|^2> = \varepsilon^2 \int_{-\infty}^{\infty} dk_x dk_y \; |T(\hat{n}\bullet\hat{k})|^2 \mathcal{PP}|_{\vec{k}_2=\vec{k}_1=\vec{k}} \; . \tag{31}$$

As in reference 25, we assume that the receiver beam pattern is highly directional, i.e.

$|T(\hat{n}\bullet\hat{k})|^2 \approx T_0^2 \delta(\hat{n}\bullet\hat{k}-1)$,

and write, after some calculations[25], the mean square signal level of the singly scattered waves as

$$<|V(\hat{n})|^2> \approx 2\pi\varepsilon^2 \frac{k_z}{k_f} T_0^2 k_f^2 \mathcal{PP}|_{\vec{k}_2=\vec{k}_1=\vec{k}} \; ,$$

with $\vec{k} = k_f \hat{n}$.

After substituting (30) into the above equation one has

$$\frac{<|V(\hat{n})|^2>}{T_0^2} \approx \left(\frac{\pi^2\varepsilon^2\rho_f^2 k_f k_T^4}{\rho_s^2\mu_0^2}\right) \frac{\int_{-\infty}^{\infty} d\xi \; \tilde{R}_\Theta(k_x-k_{0x}, k_y-k_{0y}, \xi) \; I^\Theta(k_x, k_y, \xi)}{k_z \; |F(k_x, k_y)|^2 \; |F(k_{0x}, k_{0y})|^2} \; . \tag{32}$$

This is the chief result of this section.The incoherently scattered intensity is seen to be proportional to the spatial spectral density function, R_Θ, (the Fourier transform of the auto-correlation function) of the material heterogeneity. This intensity is, furthermore, seen to peak whenever the incident or listening directions are close to the Rayleigh angle where $F = 0$.

We now use $(\theta_{out}, \phi_{out})$ and (θ_{in}, ϕ_{in}) to express the listening and incident directions as

$$\begin{cases} k_x = k_f n_x = k_f \sin\theta_{out}\cos\phi_{out}, \\ k_y = k_f n_y = k_f \sin\theta_{out}\sin\phi_{out}, \\ k_z = \eta_f = k_f n_z = k_f \cos\theta_{out}, \end{cases} \qquad \begin{cases} k_{0x} = k_f \sin\theta_{in}\cos\phi_{in}, \\ k_{0y} = k_f \sin\theta_{in}\sin\phi_{in}, \\ k_{0z} = \eta_f^0 = k_f \cos\theta_{in}, \end{cases} \tag{33}$$

and notice, from Eq. (6), that $F(k_x, k_y)$ is a function of θ only, to rewrite the mean square signal level of the single incoherently scattered waves in Eq. (32).

The leaky Rayleigh function $F(\theta)$ has a complex root at $\theta = \theta_{LR}$. The real part of θ_{LR} is quite close to the (regular) Rayleigh angle θ_R for solid half-space and vacuum, and the imaginary part of θ_{LR} is very small compared with the real part. So if one is interested only in the cases where both the incident and the listening directions are near the Rayleigh angle θ_R, one can write an approximate form of (32) as

$$\frac{<|V(\hat{n})|^2>}{T_0^2} \approx \left(\frac{\pi^2\varepsilon^2\rho_f^2 k_T^4}{\rho_s^2\mu_0^2}\right) \frac{\int_{-\infty}^{\infty} d\xi \; \tilde{R}_\Theta(\theta_R, \phi_{out}, \xi) \; I^\Theta(\theta_R, \phi_{out}, \xi)}{\cos\theta_R \; |F'(\theta_R)|^4 \; |\theta_{out}-\theta_{LR}|^2 \; |\theta_{in}-\theta_{LR}|^2} \; . \tag{32a}$$

Note that since θ_{LR} is complex, there will be no singularity in (32) and (32a) for real θ_{out} and θ_{in}, although the main contribution to the intensity comes from those θ_{out} and θ_{in} whose values are close to the real part of θ_{LR}. Fig. 1 shows the magnitude of the Rayleigh function $F(\theta)$ given in Eq.(9) varying with incident or out going angle. One can see that $F(\theta)$ quickly reduces to a (non-zero) minimum at the leaky Rayleigh angle θ_{LR} which is almost the same as regular Rayleigh angle θ_R as $\rho_f/\rho_s \to 0$. This is why the scattered signal level has a peak when incident and listening angles are near this critical angle.

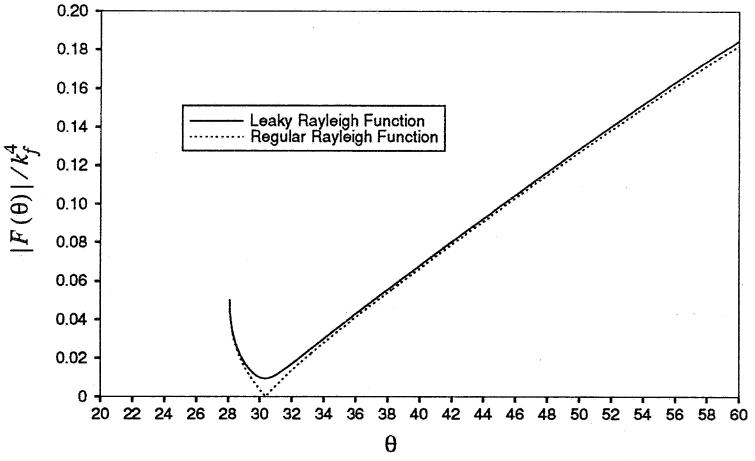

Fig. 1: Magnitude of the Rayleigh function as a function of angle for the case of an aluminum / water interface

IV A Special Case of Cubic Crystal Aggregates

In order to further simplify our result in (32), we rewrite Eq. (7) as

$$U_i(k_x, k_y; z) = U_i^L(k_x, k_y)\, e^{-\eta_L z} + U_i^T(k_x, k_y)\, e^{-\eta_T z} = \sum_{\sigma = L, T} U_i^{\sigma}(k_x, k_y)\, e^{-\eta_\sigma z} \quad , \tag{34}$$

where summation for σ is over L and T. We also rewrite (25a) as

$$J_{ij}^{MN}(k_x, k_y; z_s) = (-1)^{M+N} \sum_{\sigma_1 = L, T} \sum_{\sigma_2 = L, T} (\eta_{\sigma_1})^M (\eta_{\sigma_2}^0)^N U_i^{\sigma_1}(-k_x, -k_y)\, U_j^{\sigma_2}(k_{0x}, k_{0y})\, e^{-(\eta_{\sigma_1} + \eta_{\sigma_2}^0) z_s} \quad , \tag{35}$$

for $(M, N) = 0, 1$ and no summation convention for repeated M and N. Notice that $\eta_{L,T}^0 > 0$ for incident direction near the critical Rayleigh angle, then Eq. (30b) becomes

$$\mathcal{J}_{MNPQ}^{ijkl} = (-1)^{M+N+P+Q} \sum_{\sigma_1 = L, T} \sum_{\sigma_2 = L, T} \sum_{\sigma_3 = L, T} \sum_{\sigma_4 = L, T} (\eta_{\sigma_1})^M (\eta_{\sigma_2}^0)^N (\eta_{\sigma_3})^P (\eta_{\sigma_4}^0)^Q$$
$$\times \frac{U_i^{\sigma_1}(-k_x, -k_y)\, U_j^{\sigma_2}(k_{0x}, k_{0y})\, U_k^{\sigma_3 *}(-k_x, -k_y)\, U_l^{\sigma_4 *}(k_{0x}, k_{0y})}{(\eta_{\sigma_1} + \eta_{\sigma_2}^0 + i\xi)\,(\eta_{\sigma_3} + \eta_{\sigma_4}^0 - i\xi)} \quad . \tag{36}$$

We now consider a special case by assuming the autocovariance function $R_\Theta(\vec{r}_1 - \vec{r}_2) = R_\Theta(\vec{r})$ to be of exponential form

$$\begin{cases} R_\Theta(\vec{r}) = R_\Theta(x, y, z) = R_0 e^{-\beta|\vec{r}|} = R_0 e^{-\beta\sqrt{x^2+y^2+z^2}}, \\ \tilde{R}_\Theta(\vec{k}) = \tilde{R}_\Theta(k_x, k_y, k_z) = R_0\beta/\pi^2(\beta^2 + |\vec{k}|^2)^2 = R_0\beta/\pi^2(\beta^2 + k_x^2 + k_y^2 + k_z^2)^2. \end{cases} \tag{37}$$

Physically, β is a measure of (inversely proportional to) the average grain size[22]. We substitute (37) into (32) to obtain

$$\frac{<|V(\hat{n})|^2>}{T_0^2} \approx \left(\frac{4\varepsilon^2\rho_f^2 k_f k_T^4}{\rho_s^2\mu_0^2}\right)\frac{R_0\beta II^\Theta}{k_z\ |F(k_x, k_y)|^2\ |F(k_{0x}, k_{0y})|^2}, \tag{38}$$

with II^Θ defined as

$$II^\Theta \equiv \int_{-\infty}^{\infty} \frac{I_0^\Theta\ d\xi}{(\beta^2 + \kappa_x^2 + \kappa_y^2 + \xi^2)^2}, \tag{38a}$$

where $\kappa_{x,y} \equiv k_{x,y} - k_{0x,0y}$. I^Θ is still defined as in (30a) but with $\mathcal{I}_{MNPQ}^{ijkl}$ replaced by $\mathcal{JI}_{MNPQ}^{ijkl}$ as given in the following expression

$$\begin{aligned} \mathcal{JI}_{MNPQ}^{ijkl} &\equiv \int_{-\infty}^{\infty} \frac{\mathcal{I}_{MNPQ}^{ijkl}}{(\beta^2 + \kappa_x^2 + \kappa_y^2 + \xi^2)^2} d\xi, \\ &= \frac{\pi}{2}(-1)^{M+N+P+Q} \sum_{\sigma_1=L,T}\sum_{\sigma_2=L,T}\sum_{\sigma_3=L,T}\sum_{\sigma_4=L,T} (\eta_{\sigma_1})^M (\eta_{\sigma_2}^0)^N (\eta_{\sigma_3})^P (\eta_{\sigma_4}^0)^Q \\ &\quad \times \frac{U_i^{\sigma_1}(-k_x, -k_y)\, U_j^{\sigma_2}(k_{0x}, k_{0y})\, U_k^{\sigma_3 *}(-k_x, -k_y)\, U_l^{\sigma_4 *}(k_{0x}, k_{0y})}{(\beta^2 + \kappa_x^2 + \kappa_y^2)^{3/2}\ [\eta_{\sigma_1} + \eta_{\sigma_2}^0 + \eta_{\sigma_3} + \eta_{\sigma_4}^0]} \\ &\quad \times \left\{ \frac{2\sqrt{\beta^2 + \kappa_x^2 + \kappa_y^2} + (\eta_{\sigma_1} + \eta_{\sigma_2}^0)}{\left[\sqrt{\beta^2 + \kappa_x^2 + \kappa_y^2} + (\eta_{\sigma_1} + \eta_{\sigma_2}^0)\right]^2} + \frac{2\sqrt{\beta^2 + \kappa_x^2 + \kappa_y^2} + (\eta_{\sigma_3} + \eta_{\sigma_4}^0)}{\left[\sqrt{\beta^2 + \kappa_x^2 + \kappa_y^2} + (\eta_{\sigma_3} + \eta_{\sigma_4}^0)\right]^2} \right\}. \end{aligned} \tag{38b}$$

One can further non-dimensionalize the received signal intensity in (38) by noticing that $F(k_x, k_y)/k_f^4$ is a function of θ, ρ_f/ρ_s, and $c_f/c_{L,T}$ but independent of frequency ω and ϕ. So if one is interested only for the case of incident and listening on the Rayleigh conic, that is $\theta_{in} = \theta_{out} = Re(\theta_{LR}) \approx \theta_R$, one can define the non-dimensionalized signal intensity $|\mathcal{V}(\hat{n})|^2$ as

$$|\mathcal{V}(\hat{n})|^2 \equiv \frac{<|V(\hat{n})|^2>}{4T_0^2}\frac{\mu_0^2}{\varepsilon^2 R_0}. \tag{39}$$

From (38), one has

$$|\mathcal{V}(\hat{n})|^2 \approx \frac{\rho_f^2 c_f^4}{\rho_s^2 c_T^4}\left(\frac{\beta}{k_f}\right)\frac{k_f^5\ \Pi^{\Theta}(\theta_R, \phi_{out}, \beta/k_f, c_f/c_L, c_f/c_T)}{\cos\theta_R |F(\theta_R)|^4}\ , \tag{40}$$

which is a function of k_f/β, ρ_f/ρ_s, c_f/c_L and c_f/c_T only (θ_R is a function of the last three dimensionless parameters).

Now we consider two limiting cases.

In the Rayleigh (low frequency) limit where $k_f/\beta \ll 1$, one finds from (38b) and (40) that the mean square incoherently scattered signal level $|\mathcal{V}(\hat{n})|^2$ is proportional to a sum of terms of order $(k_f/\beta)^3$. On the other hand, in the geometrical optics (high frequency) limit where $k_f/\beta \gg 1$, $|\mathcal{V}(\hat{n})|^2$ is inversely proportional to the dimensionless frequency k_f/β.

These behaviors can be better understood by recognizing that the diffusely scattered intensity should be proportional to the ratio of the attenuation of a Rayleigh wave due to scattering to the attenuation due to leaking. That is, the diffusely scattered intensity should be proportional to the probability that the wave scatters before it leaks. Attenuation due to leaking scales with the 1st power of frequency. Attenuation due to scattering scales, in the Rayleigh limit, with the 4th power of frequency[23], and in the geometrical optics limit, independent of ω (or the dimensionless k_f/β). The ratios of these attenuations to leaking are then of the 3rd and inverse power of frequency respectively.

V Numerical Results for Cubic Crystal Aggregates

For equiaxed cubic crystal aggregates, $R_0 = \zeta^2$ where ζ is the anisotropic factor. The eighth rank isotropic tensor $\Xi_{ijkl}^{\alpha\beta\gamma\delta}$ is invariant under any permutation of greek and/or latin indices. It can be constructed totally from Kronecker deltas in the form[24]

$$\begin{aligned}\Xi_{ijkl}^{\alpha\beta\gamma\delta} = {} & b(\delta_{\alpha\beta}\delta_{\gamma\delta}+\delta_{\alpha\gamma}\delta_{\beta\delta}+\delta_{\alpha\delta}\delta_{\beta\gamma})(\delta_{ij}\delta_{kl}+\delta_{ik}\delta_{jl}+\delta_{il}\delta_{jk}) \\ & + d\{\delta_{\alpha i}\delta_{\beta j}\delta_{\gamma\delta}\delta_{kl} + \textit{all the permutations consisting of exactly two pairings between greek and latin indices, one pairing between greek and greek indices, and one pairing between latin and latin indices}\} \\ & + h\{\delta_{\alpha i}\delta_{\beta j}\delta_{\gamma k}\delta_{\delta l} + \textit{all the permutations consisting of exactly four pairings between greek and latin indices}\}.\end{aligned} \tag{41}$$

The numerical coefficients b, d and h can be determined by evaluating three independent components of Ξ, and are found to be[22]

$$b = 2/1575, \qquad d = -1/630, \qquad h = 1/180. \tag{42}$$

Using (41) and (42), one can calculate that the non-zero components of tensor $\Xi_{ijkl}^{\alpha\beta\gamma\delta}$ are

$$
\begin{cases}
\Xi_{1111}^{1111} = \Xi_{2222}^{2222} = \Xi_{3333}^{3333} = 9b + 72d + 24h = 16/525, \\
\Xi_{2222}^{1111} = \Xi_{3333}^{2222} = \Xi_{1111}^{3333} = 9b = 2/175, \\
\Xi_{1122}^{1111} = \Xi_{1133}^{1111} = \Xi_{1122}^{2222} = \Xi_{2233}^{2222} = \Xi_{1133}^{3333} = \Xi_{2233}^{3333} = 3b + 12d = -8/525, \\
\Xi_{2233}^{1111} = \Xi_{1133}^{2222} = \Xi_{1122}^{3333} = 3b = 2/525, \\
\Xi_{1122}^{1122} = \Xi_{2233}^{2233} = \Xi_{1133}^{1133} = b + 4d + 4h = 3/175, \\
\Xi_{1133}^{1122} = \Xi_{2233}^{1122} = \Xi_{1122}^{2233} = \Xi_{1133}^{2233} = b + 2d = -3/525, \\
\Xi_{1112}^{1112} = \Xi_{1113}^{1113} = \Xi_{1222}^{1222} = \Xi_{2223}^{2223} = \Xi_{1333}^{1333} = \Xi_{2333}^{2333} = 9d + 6h = 2/105, \\
\Xi_{1123}^{1123} = \Xi_{1223}^{1223} = \Xi_{1233}^{1233} = d + 2h = 1/105, \\
\Xi_{1222}^{1112} = \Xi_{1333}^{1113} = \Xi_{2333}^{2223} = 9d = -3/210, \\
\Xi_{1233}^{1112} = \Xi_{1233}^{1222} = \Xi_{1223}^{1113} = \Xi_{1223}^{1333} = \Xi_{1123}^{2223} = \Xi_{1123}^{2333} = 3d = -1/210.
\end{cases}
\tag{43}
$$

One also has the relation $\Xi_{ijkl}^{\alpha\beta\gamma\delta} = \Xi_{\alpha\beta\gamma\delta}^{ijkl}$ and all permutations within upper or lower indexes keep the value unchanged. All other components that contain at least one index (upper or lower) being repeated of odd number of times are zero.

For water-aluminum case, one has $\rho_f/\rho_s = 0.3696$, $c_f/c_L = 0.23726$, and $c_f/c_T = 0.47106$. From (6), one find that $\theta_{LR} \approx \theta_R \approx 30.36^o$. Plotted in Fig. 1 are the magnitude of the dimensionless leaky Rayleigh function given in (6) and that of the regular Rayleigh function (Eq. (6) with $\rho_f/\rho_s = 0$) as functions of (the incident or outgoing) angle θ. One can see that both critical angles (corresponding the minimum) have approximately the same value.

Plotted in Fig.2 is the numerical results given by Eq. (40) for the backscattered signal ($\phi_{out} = 180^o$). One can see from this plot, as discussed in last section, at high frequency (geometrical) limit, the mean square scattered signal level is inversely proportional to the non-dimensional frequency. In the low frequency (Rayleigh) limit, the mean square scattered signal level is proportional to the third power of frequency.

Similar frequency dependence relationships are also found for the out of plane scattered signals, but the turning point between the frequency regimes alters with ϕ_{out}, as can be seen from Fig. 3. The turning point decreases with the increase of the out of plane listening angle from $\phi_{out} = 0^o$ (forward scattering) to $\phi_{out} \approx 90^o$ (completely out of plane scattering) and then remains about the same at $k_f/\beta \approx 1.0$ for all ϕ_{out} from 90^o to 180^o (backward scattering).

Fig.4 is a plot of the mean square scattered signal level as a function of the listening direction (angles θ_{out} and ϕ_{out}) at low frequency ($k_f/\beta = 0.1$). One can see that a peak near $\theta_R \approx 30.3^o$ exists

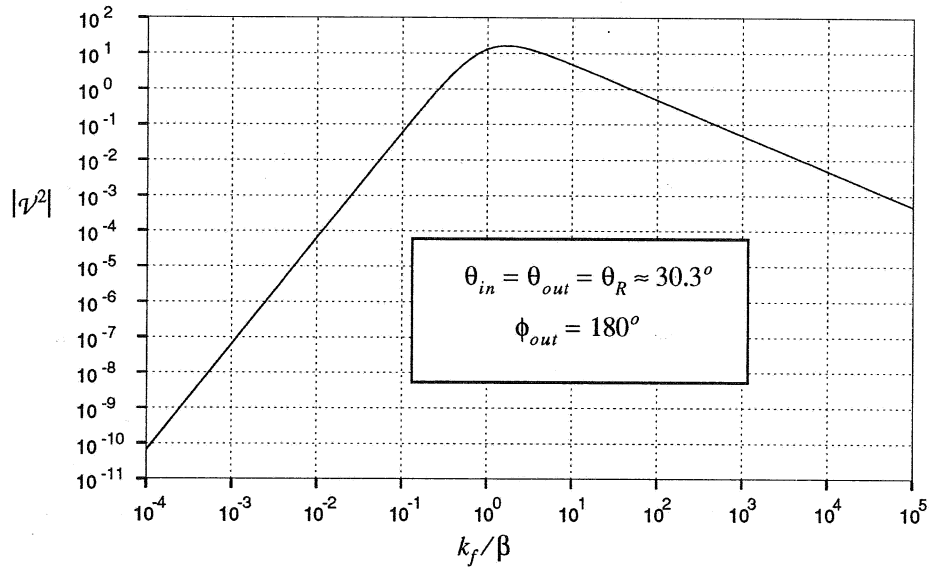

Fig. 2: Backscattered mean square signal level as a function of frequency

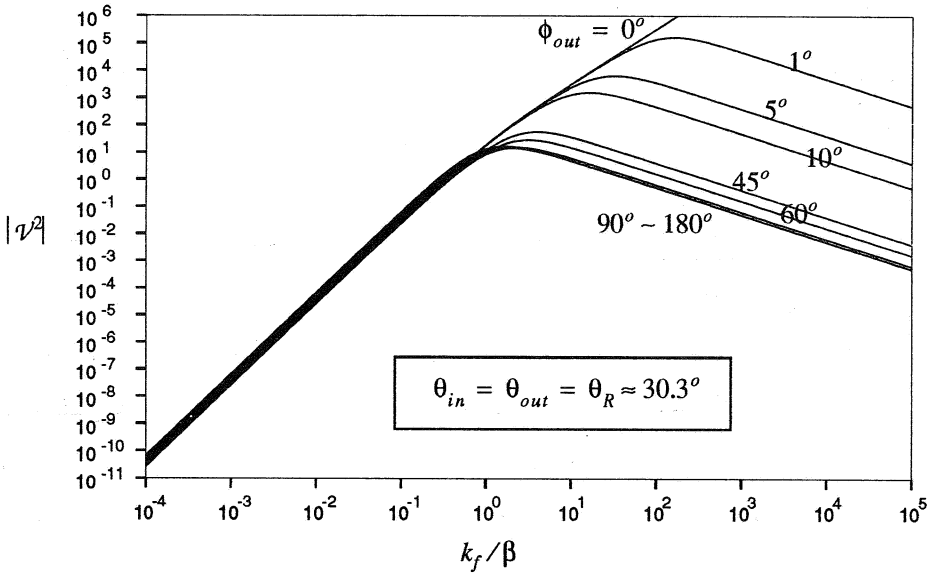

Fig. 3: Mean square scattered signal level as a function of frequency and for different off plane listening angle

for every ϕ_{out} but the backscattered signal ($\phi_{out} = 180^o$) is about twice as strong as the forward scattered signal ($\phi_{out} = 0^o$).

In the high frequency situation, the picture is different. Because of the turning point from cubic frequency dependence to inverse proportionality comes late at higher frequencies for small ϕ_{out}, the difference between the forward scattered mean square signal level and the backward scat-

tered mean square signal level is very big. The reason can be seen from Eq. (38b). For high frequencies, k_f/β is large, one can approximate that $\beta \to 0$ in (38b) and find $(k_f/\beta)^{-1}$ dependence as described in last section. But if near the forward direction ($\theta_{out} = \theta_{in}$ and $\phi_{out} = 0^o$) one find that $\kappa_x \approx 0$ and $\kappa_y \approx 0$, then $\beta^2 + \kappa_x^2 + \kappa_y^2 \approx \beta^2$ so that cubic frequency dependence relationship still holds in or near this forward direction, as can be seen from Fig.3.

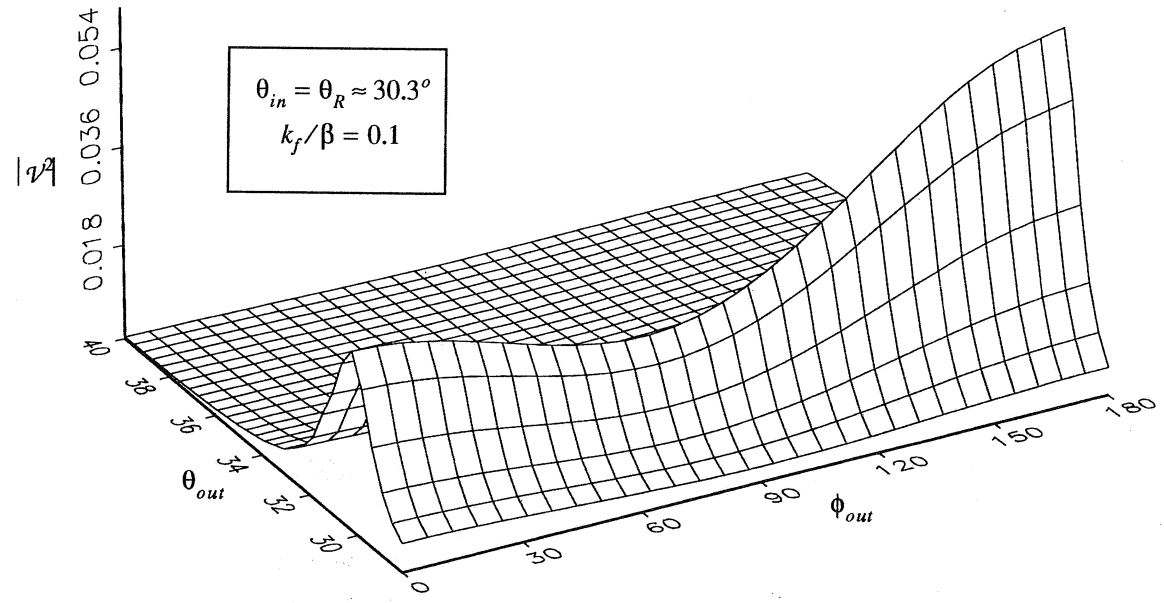

Fig. 4: Mean square scattered signal level as a function of the listening direction at low frequency

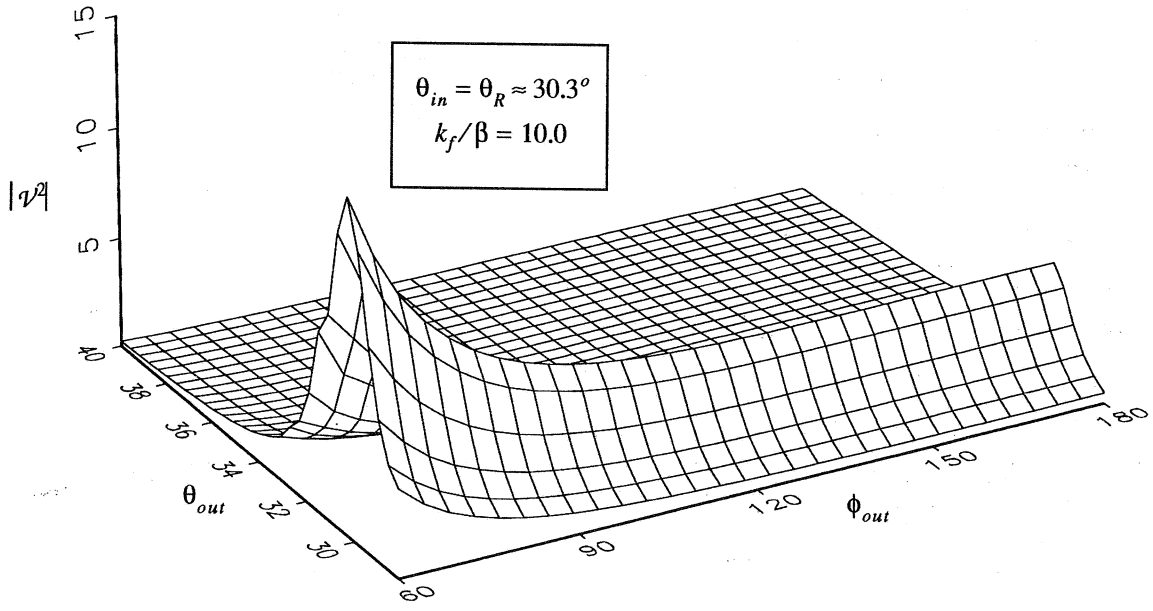

Fig. 5: Mean square scattered signal level as a function of the listening direction at high frequency

Fig.5 shows that for high frequency, the mean square scattered signal level remains about the same for different ϕ_{out} between $90^o \sim 180^o$. Also for fixed ϕ_{out}, the scattered signal is strongest when θ_{out} is near θ_R.

Plotted in Fig.6 is the mean square scattered signal level as a function of ϕ_{out} at high frequency and when $\theta_{out} = \theta_R$. It covers the full range of ϕ_{out} from $\phi_{out} = 0^o$ (forward direction) to $\phi_{out} = 180^o$ (backward direction) at the Rayleigh angle while in Fig. 5, $60^o \leq \phi_{out} \leq 180^o$.

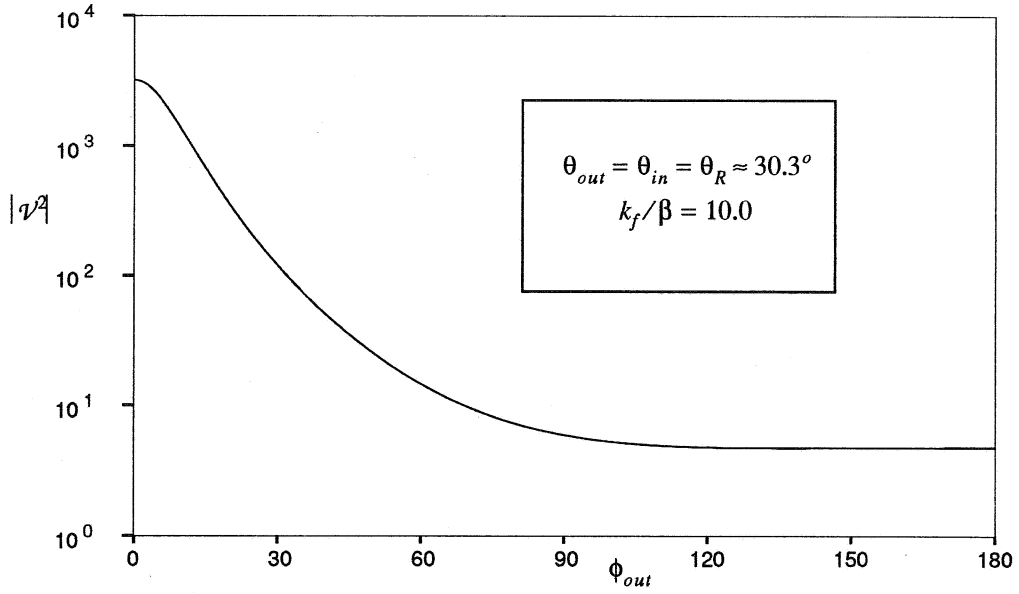

Fig. 6: Mean square scattered signal level as a function of the off plane listening angle at high frequency

VI Summary and Conclusions

A first order Born approximation is utilized to obtain the incoherent scattering from a flat fluid-solid interface. The fluid is assumed to be ideal and homogeneous, but the solid has randomly inhomogeneous anisotropic elastic constants due to the microstructure of the material. A harmonic plane wave is incident from the fluid on to the interface and the mean square scattered signal level is given in terms of an integration of the spatial spectral density (the spatial Fourier transform of the auto-covariance function of the fluctuating elastic moduli). The principle of reciprocity is also utilized to make the calculations simpler.

For the case of exponential type auto-covariance function, the integration can be calculated easily and the final analytic result is given. The results for the high and low frequency limits can be readily seen from the analytical formula. For high frequency (geometrical) limit, the mean

square scattered signal level is found to be inversely proportional to frequency, while for the low frequency (Rayleigh) limit, a cubic power frequency dependence is found. Physical explanations are given for these frequency dependences.

Numerical results are given for the case of a cubic polycrystalline aggregate (Aluminum) at a water interface. These numerical results show, in addition to the verification of the analytical predictions of the frequency dependences mentioned above, that at low frequencies, the mean square scattered signal level in the backward direction is as twice as that of the forward direction while the weakest scattering is in the out of (the incident) plane directions. At high frequencies, the mean square scattered signal level remains about the same for all the out of (the incident) plane angles which are greater than 90^0 (backward like).

Acknowledgment

The support by the National Science Foundation Solid Mechanics Program through grant number MSS-91-14360 is gratefully acknowledged.

References

[1] W.M.Ewing, W.S.Jardetzky and F.Press, *Elastic Waves in Layered Media*, McGraw-Hill, New York (1957)

[2] L.M.Brekhovskikh, *Waves in Layered Media*, Academic Press, New York (1960)

[3] I.A.Victorov, *Rayleigh and Lamb Waves*, Plenum, New York (1967)

[4] F.L.Becker and R.L.Richardson, Ultrasonic critical angle reflectivity, in *Research Techniques in Nondestructive Testing*, edited by R.S.Sharpe, Academic Press, New York (1970), pp 91-131

[5] G.W.Farnell, Properties of elastic surface waves, in *Physical Acoustics*, edited by W.P.Mason and R.N.Thurston, Academic Press, New York, Vol. VI (1970), pp 109-166

[6] K.Dransfeld and E.Salzmann, Excitation, detection, and attenuation of high-frequency elastic surface waves, in *Physical Acoustics*, edited by W.P.Mason and R.N.Thurston, Academic Press, New York, Vol. VII (1970), pp 219-272

[7] H. Überal, Surface waves in acoustics, in *Physical Acoustics*, edited by W.P.Mason and R.N.Thurston, Academic Press, New York, Vol. X (1973), pp 1-60

[8] G.W.Farnell, Types and properties of surface waves, in *Acoustic Surface Waves*, edited by A.A.Oliner, Springer-Verlag, New York (1978), pp 13-60

[9] A.A.Oliner, Introduction, in *Acoustic Surface Waves*, edited by A.A.Oliner, Springer-Verlag, New York (1978), pp 1-11

[10] F.R.Rollins,Jr, Critical ultrasonic reflectivity - A neglected tool for material evaluation, *Mat. Eval.*, **24**, 683-689, 1966

[11] M.G.Silk, Relationships between metallurgical texture and ultrasonic propagation, *Metal. Sci.*, **15**, 559-565, 1981

[12] G.T.Curtis and N.Ibrahim, Texture studies of austenitic weld metal using elastic surface wave, *Metal. Sci.*, **15**, 566-573, 1981

[13] D.Husson, S.S.Bennet and G.S.Kino, Measurement of stress with surface waves, *Mat. Eval.*, **43**(1), 92-100, 1985

[14] P.P.Delsanto and A.V.Clark,Jr., Rayleigh wave propagation in deformed orthotropic materials, *J. Acoust. Soc. Am.*, **81**(4), 952-960, 1987

[15] P.P.Delsanto, R.B.Mignogna and A.V.Clark,Jr., Ultrasonic texture and stress measurements in anisotropic polycrystalline aggregates, *J. Acoust. Soc. Am.*, **87**(1), 215-224, 1990

[16] J.L.Rose, A.Nayfeh and A.Pilarski, Surface waves for material characterization, *Trans. ASME, J. Appl. Mech.*, **57**, 7-11, 1990

[17] B.R.Tittmann, F.Cohen, Tennoudji, M.de Billy, A.Jungmann & G.Quentin, A simple approach to estimate the size of small surface cracks with the use of acoustic surface waves, *Appl. Phys. Lett.*, **33**(1), 6-8, 1973

[18] A.Klein & H.J.Salzburger, Characterization of surface defects by Rayleigh-waves, in New Procedures in Nondestructive Testing, edited by P.Höller, Springer-Verlag, Berlin (1983), pp 193-202

[19] T.M.Hsieh and M.Rosen, Ultrasonic leaky waves for non-destructive interface characterization, *Ultrasonics*, **31**(1), 45-51, 1993

[20] Y.C.Fung, *Foundations of Solid Mechanics*, Prentice-Hall, Inc., Englewood Cliffs, NJ (1965), pp 429-432

[21] J.D.Achenbach, *Wave Propagation in Elastic Solids*, (North-Holland Publishing Company, NY, 1973), pp 82-85

[22] A.A.Maradudin & D.L.Mills, The attenuation of Rayleigh surface waves by surface roughness, Annals of Phys., 100, 262-309, 1976

[23] I.M.Kaganova & A.A.Maradudin, Surface acoustic waves on a polycrystalline substrate, *Physica Scripta*, **T44**, 104-112, 1992

[23] R.L.Weaver, Diffusivity of ultrasound in polycrystals, *J. Mech. Phys. Solids*, **38**(1), 55-86, 1990

[24] Y.Zhang & R.L.Weaver, Scattering from a random fluid layer, *J. Acoust. Soc. Am.*, **96**(3), 1994 (to appear)

List of Recent TAM Reports

No.	Authors	Title	Date
712	Cherukuri, H. P., and T. G. Shawki	An energy-based localization theory: Part I—Basic framework	Apr. 1993
713	Manring, N. D., and R. E. Johnson	Modeling a variable-displacement pump	June 1993
714	Birnbaum, H. K., and P. Sofronis	Hydrogen-enhanced localized plasticity—A mechanism for hydrogen-related fracture	July 1993
715	Balachandar, S., and M. R. Malik	Inviscid instability of streamwise corner flow	July 1993
716	Sofronis, P.	Linearized hydrogen elasticity	July 1993
717	Nitzsche, V. R., and K. J. Hsia	Modelling of dislocation mobility controlled brittle-to-ductile transition	July 1993
718	Hsia, K. J., and A. S. Argon	Experimental study of the mechanisms of brittle-to-ductile transition of cleavage fracture in silicon single crystals	July 1993
719	Cherukuri, H. P., and T. G. Shawki	An energy-based localization theory: Part II—Effects of the diffusion, inertia and dissipation numbers	Aug. 1993
720	Aref, H., and S. W. Jones	Chaotic motion of a solid through ideal fluid	Aug. 1993
721	Stewart, D. S.	Lectures on detonation physics: Introduction to the theory of detonation shock dynamics	Aug. 1993
722	Lawrence, C. J., and R. Mei	Long-time behavior of the drag on a body in impulsive motion	Sept. 1993
723	Mei, R., J. F. Klausner, and C. J. Lawrence	A note on the history force on a spherical bubble at finite Reynolds number	Sept. 1993
724	Qi, Q., R. E. Johnson, and J. G. Harris	A re-examination of the boundary layer attenuation and acoustic streaming accompanying plane wave propagation in a circular tube	Sept. 1993
725	Turner, J. A., and R. L. Weaver	Radiative transfer of ultrasound	Sept. 1993
726	Yogeswaren, E. K., and J. G. Harris	A model of a confocal ultrasonic inspection system for interfaces	Sept. 1993
727	Yao, J., and D. S. Stewart	On the normal detonation shock velocity–curvature relationship for materials with large activation energy	Sept. 1993
728	Qi, Q.	Attenuated leaky Rayleigh waves	Oct. 1993
729	Sofronis, P., and H. K. Birnbaum	Mechanics of hydrogen–dislocation–impurity interactions: Part I—Increasing shear modulus	Oct. 1993
730	Hsia, K. J., Z. Suo, and W. Yang	Cleavage due to dislocation confinement in layered materials	Oct. 1993
731	Acharya, A., and T. G. Shawki	A second-deformation-gradient theory of plasticity	Oct. 1993
732	Michaleris, P., D. A. Tortorelli, and C. A. Vidal	Tangent operators and design sensitivity formulations for transient nonlinear coupled problems with applications to elasto-plasticity	Nov. 1993
733	Michaleris, P., D. A. Tortorelli, and C. A. Vidal	Analysis and optimization of weakly coupled thermo-elasto-plastic systems with applications to weldment design	Nov. 1993
734	Ford, D. K., and D. S. Stewart	Probabilistic modeling of propellant beds exposed to strong stimulus	Nov. 1993
735	Mei, R., R. J. Adrian, and T. J. Hanratty	Particle dispersion in isotropic turbulence under the influence of non-Stokesian drag and gravitational settling	Nov. 1993
736	Dey, N., D. F. Socie, and K. J. Hsia	Static and cyclic fatigue failure at high temperature in ceramics containing grain boundary viscous phase: Part I—Experiments	Nov. 1993
737	Dey, N., D. F. Socie, and K. J. Hsia	Static and cyclic fatigue failure at high temperature in ceramics containing grain boundary viscous phase: Part II—Modelling	Nov. 1993

(continued on next page)

List of Recent TAM Reports (cont'd)

No.	*Authors*	*Title*	*Date*
738	Turner, J. A., and R. L. Weaver	Radiative transfer and multiple scattering of diffuse ultrasound in polycrystalline media	Nov. 1993
739	Qi, Q., and R. E. Johnson	Resin flows through a porous fiber collection in pultrusion processing	Dec. 1993
740	Weaver, R. L., W. Sachse, and K. Y. Kim	Transient elastic waves in a transversely isotropic plate	Dec. 1993
741	Zhang, Y., and R. L. Weaver	Scattering from a thin random fluid layer	Dec. 1993
742	Weaver, R. L., and W. Sachse	Diffusion of ultrasound in a glass bead slurry	Dec. 1993
743	Sundermeyer, J. N., and R. L. Weaver	On crack identification and characterization in a beam by nonlinear vibration analysis	Dec. 1993
744	Li, L., and N. R. Sottos	Predictions of static displacements in 1–3 piezocomposites	Dec. 1993
745	Jones, S. W.	Chaotic advection and dispersion	Jan. 1994
746	Stewart, D. S., and J. Yao	Critical detonation shock curvature and failure dynamics: Developments in the theory of detonation shock dynamics	Feb. 1994
747	Mei, R., and R. J. Adrian	Effect of Reynolds-number-dependent turbulence structure on the dispersion of fluid and particles	Feb. 1994
748	Liu, Z.-C., R. J. Adrian, and T. J. Hanratty	Reynolds-number similarity of orthogonal decomposition of the outer layer of turbulent wall flow	Feb. 1994
749	Barnhart, D. H., R. J. Adrian, and G. C. Papen	Phase-conjugate holographic system for high-resolution particle image velocimetry	Feb. 1994
750	Qi, Q., W. D. O'Brien Jr., and J. G. Harris	The propagation of ultrasonic waves through a bubbly liquid into tissue: A linear analysis	Mar. 1994
751	Mittal, R., and S. Balachandar	Direct numerical simulation of flow past elliptic cylinders	May 1994
752	Anderson, D. N., J. R. Dahlen, M. J. Danyluk, A. M. Dreyer, K. M. Durkin, J. J. Kriegsmann, J. T. McGonigle, and V. Tyagi	Thirty-first student symposium on engineering mechanics, J. W. Phillips, coord.	May 1994
753	Thoroddsen, S. T.	The failure of the Kolmogorov refined similarity hypothesis in fluid turbulence	May 1994
754	Turner, J. A., and R. L. Weaver	Time dependence of multiply scattered diffuse ultrasound in polycrystalline media	June 1994
755	Riahi, D. N.	Finite-amplitude thermal convection with spatially modulated boundary temperatures	June 1994
756	Riahi, D. N.	Renormalization group analysis for stratified turbulence	June 1994
757	Riahi, D. N.	Wave-packet convection in a porous layer with boundary imperfections	June 1994
758	Jog, C. S., and R. B. Haber	Stability of finite element models for distributed-parameter optimization and topology design	July 1994
759	Qi, Q., and G. J. Brereton	Mechanisms of removal of micron-sized particles by high-frequency ultrasonic waves	July 1994
760	Shawki, T. G.	On shear flow localization with traction-controlled boundaries	July 1994
761	Balachandar, S., D. A. Yuen, and D. M. Reuteler	High Rayleigh number convection at infinite Prandtl number with temperature-dependent viscosity	July 1994
762	Phillips, J. W.	Arthur Newell Talbot—Proceedings of a conference to honor TAM's first department head and his family	Aug. 1994
763	Man., C. S., and D. E. Carlson	On the traction problem of dead loading in linear elasticity with initial stress	Aug. 1994
764	Zhang, Y., and R. L. Weaver	Leaky Rayleigh wave scattering from elastic media with random microstructures	Aug. 1994